

U.S. Department of Commerce
National Oceanic and Atmospheric Administration
National Weather Service
National Centers for Environmental Prediction
5830 University Research Court
College Park, MD 20740-3818

Office Note 499

<https://doi.org/10.25923/xrzp-x016>

A FORMULATION OF THE HEXAD ALGORITHM USING THE GEOMETRY
OF THE FANO PROJECTIVE PLANE

R. James Purser*
IM Systems Group, Rockville, Maryland

January 30, 2020

THIS IS AN UNREVIEWED MANUSCRIPT, PRIMARILY INTENDED FOR INFORMAL
EXCHANGE OF INFORMATION AMONG THE NCEP STAFF MEMBERS

* email: jim.purser@noaa.gov

Abstract

In what we call the ‘Hexad Algorithm’, for anisotropic variational data assimilation, a spatial covariance’s second moment, or ‘aspect tensor’, is decomposed at each location of a spatial computational lattice into six generalized grid line rank-one components (‘aspect weights’) that linearly recombine to form the original tensor. The selection of the six line directions is effected by an iterative procedure that is essentially a specialized variant of the classical Simplex Algorithm of linear programming theory. The ‘hexads’, or sets of six integer 3-vector generators that define these line orientations, must conform to a particular fixed set of linear relationships amongst them in order to be valid. Hence, these relationships implicitly govern the way one hexad can transition through a change in a single generator to a neighboring hexad in the network they collectively constitute. The central task of the Hexad Algorithm is to guide each incremental step of this iterative search through the network of the valid hexads, seeking the desired configuration (which, apart from borderline cases, is unique) in which the implied six aspect weights are all nonnegative. Six one-dimensional smoothing operators, applied sequentially and each contributing its prescribed rank-one share, then enable a computationally efficient approximation of the effect of convolving gridded data with a locally quasi-Gaussian kernel that possesses, in its spatial second moment, the intended aspect tensor.

The otherwise formidable combinatorial complexities involved at each step of the Hexad Algorithm are made more manageable whenever it becomes possible to exploit geometrical symmetries. These are conveniently supplied through a natural mapping from each of the possible line generators that can participate in the Hexad Algorithm to the set of seven nonnull elements of the Galois field, $GF(8)$, of abstract algebra, with each member of the hexad mapping to a different element of that field. The Galois field elements in turn are associated with the seven ‘points’ of the finite projective geometry known as the ‘Fano plane’. We show, by exploiting the symmetries implied by these abstract algebraic structures, that the coded algorithm resolving each aspect tensor into its hexad of rank-one components achieves a particularly simple and elegant form.

1. INTRODUCTION

The Triad and Hexad algorithms were methods proposed as ways to efficiently generate controlled anisotropic quasi-Gaussian smoothing filters in two and three dimensions respectively when the fundamental smoothing operations were the one-dimensional recursive line filters of Purser and McQuigg (1982), Hayden and Purser (1995), Wu et al. (2002), Purser et al. (2003a). These quasi-Gaussian filters could then be combined, by a positive superposition at a spectrum of different spatial scales, to serve as smooth background covariance operators. The resulting anisotropic filter algorithms, as described in Purser et al. (2003b), regulated the order of application of the sequential line operations organized into batches according to what were referred to as their ‘colors’. These colors were determined as follows. The ‘generator’ (shortest integer vector) that pointed along the direction of application of a given line smoother, when its components were reduced modulo-2, were noticed to always be one of three kinds in the two-dimensional (2D) case, or of seven kinds in the three-dimensional (3D) case, which were notionally regarded to be the ‘colors’ of each line of the triad and hexad. It was also noted that, in the 2D case, every well-formed triad consisted of a set of lines whose generators could be summed to zero and had a representative of each of the three colors. In the 3D case, the six generators of the hexad had a more complicated set of geometrical relationships, but still always had six distinct colors. Therefore, in the 3D case, the hexad as a whole could always be uniquely associated with the single color of the palette of seven that was *not* represented amongst its generators.

Now, since the line operators of each triad or hexad needed to be executed in some serial order, and it was important that the line operators at one stage of the sequence did not cross another line whose own operation was not yet completed, the organization of this sequence of operations by colors ensured that such collisions could never occur. These methods were referred to as the ‘Chromatic Triad’ and ‘Chromatic Hexad’ algorithms accordingly, and it was soon realized that such an association of distinct labels of three possible ‘colors’ in the simplest implementation of the 2D case, and seven in the 3D case, actually related to the distinct non-null elements of the finite fields, or ‘Galois fields’, $GF(4)$ and $GF(8)$, of abstract algebra, as determined by just the additive properties of these fields. (The operational 2D version used in the Real-Time Mesoscale Analysis (RTMA; see de Pondeca et al., 2011) actually uses a slightly more sophisticated ‘Blended Triads’ algorithm to preserve smoothness, and this requires four colors which can be associated with another Galois field, $GF(9)$; the replacement of the recursive filters by the new beta filters removes the need of this added degree of sophistication.)

A finite field also has a multiplicative and commutative (‘Abelian’) group structure. Moreover, the multiplications (excluding the null element, of course) of a finite field always form a cyclic group. It has since been realized that, in 3D and in 4D (where the relevant field is $GF(16)$, with 15 non-null elements), the exploitation of the cyclic attribute of the group of multiplicative elements of these non-null elements can appreciably simplify the structure of the Hexad algorithm itself. In fact, for the far more complicated 4D ‘Decad algorithm’, that we shall treat in a companion note (Purser, 2020), the use of this attribute becomes practically indispensable.

2. THE FANO PLANE

The cursory description of the particular implementation of the Hexad method in Purser et al. (2003b) was given before the value of exploiting the multiplicative and cyclic attributes of the associated Galois field was recognized. Very closely related to the topic of finite fields is that of finite projective geometries. These were first introduced by Fano (1892) at about the time when Klein, Hilbert, Peano, Frege and other mathematicians of the period were engaged in the establishment of the axiomatic foundations of arithmetic and geometry. The simplest and most celebrated of Fano's 'geometries' is the one comprising just seven 'points' and seven 'lines'. This is normally referred to as *the Fano plane* (although he introduced many other finite geometries besides this simplest example). In their classic study, Veblen and Bussey (1906) expanded the study of finite projective geometries to those associated with a wider class of the Galois fields, introducing a notation ' $PG(d, p)$ ' for such geometries in d -dimensions with a prime-base p for the Galois field. In this notation, which has become standard, the Fano plane corresponds to $PG(2, 2)$. In order to motivate the construction of the Fano plane we therefore begin with the construction of the Galois field that it is associated with.

Suppose we project the infinite lattice of integer 3-vectors, by a reduction of their components, modulo-2. We can regard each resulting 3-vector of zeros and ones as providing the coefficients of a quadratic polynomial. One of the possible nonzero vectors serves as the 'identity', say $g_0(z) = (1, 0, 0) \equiv 1 + 0z + 0z^2$. Then we can consider the effect of repeatedly multiplying by some other 'polynomial', say, $g_1(z) = (0, 1, 0) \equiv 0 + 1z + 0z^2$, subject to the additional assumption of the existence of an effective 'polynomial modulus',

$$P(z) = 1 + z + z^3 \equiv 0. \quad (2.1)$$

In other words, we permit ourselves to extend the idea of modular arithmetic to the case where a nontrivial cubic polynomial becomes equivalent to the additive identity, $\mathbf{0}$, so that our set of interacting distinct polynomials need only consist of terms up to quadratic. Then the sequence of polynomial multiplications applied modulo-2 (component-wise) and modulo- $P(z)$ (for each whole polynomial), leads to the following cyclic sequence of implied polynomials:

$$g_0(z) = (1, 0, 0) \quad (2.2a)$$

$$g_1(z) = (0, 1, 0) \quad (2.2b)$$

$$g_2(z) = (0, 0, 1) \quad (2.2c)$$

$$g_3(z) = (1, 1, 0) \quad (2.2d)$$

$$g_4(z) = (0, 1, 1) \quad (2.2e)$$

$$g_5(z) = (1, 1, 1) \quad (2.2f)$$

$$g_6(z) = (1, 0, 1). \quad (2.2g)$$

Clearly, any generalized grid line generator, an irreducible[†] integer 3-vector, \mathbf{g} , after being reduced modulo-2 to a 3-vector of only ones and zeros, can be matched with one of these polynomials, g_k , and hence can take the polynomial's suffix k as its own characteristic 'color'.

[†] An integer vector is 'irreducible' if there exists no common divisor of all its components

Note that, modulus conditions on the construction of our polynomials do not invalidate the associative and commutative laws governing the multiplicative operation that the g_k can be considered to inherit, so the color indices, k , serve as effective ‘logarithms’ that behave additively (modulo-7) when the elements g_k multiply.

The multiplications of our septet of polynomials form a representation of the cyclic group, C_7 . The various linearly-dependent triples, which we can call the ‘triads’ (since they behave exactly as they would be expected to in the Triad algorithm), are the sets of the form:

$$\mathcal{L}_j = \{g_{j+1}, g_{j+2}, g_{j+4}\}, \quad (2.3)$$

(index additions implicitly modulo-7), the cyclic index pattern being exactly what we shall see to provide the definition of the ‘lines’ of the Fano plane $PG(2, 2)$. Similarly, the generators of the hexad whose colors conform to this same (+1, +2, +4) pattern of indices are found also to be linearly dependent triads. In a given hexad, the particular triad whose generator indices correspond to the Fano ‘points’ of the unique Fano ‘line’ that has the same index as the hexad’s own ‘color’ will be denoted that hexad’s ‘L-set’. To summarize, the four triads of a given hexad correspond to some of the ‘lines’ of the Fano plane, and one of these four triads (the ‘L-set’ triad), regarded as a Fano ‘line’ has the same index as the color of the hexad itself.

This self-dual geometry is shown in a version of its conventional presentation in Fig. 1, with its seven points (labeled from g_0 to g_6 in the small disks) and seven lines that link triplets of these points (drawn as the connecting lines or curves, and which it is also convenient to number from 0 to 6).

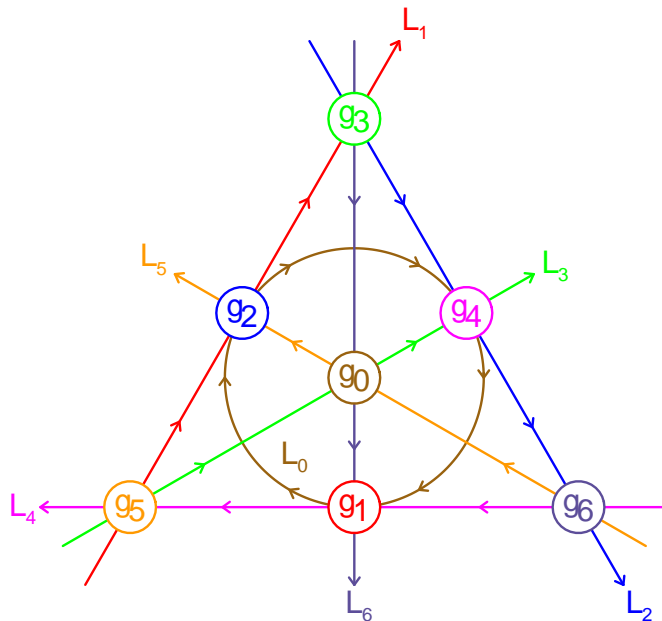


Figure 1. A conventional depiction of the Fano plane with seven points (g_i , shown by the small colored rings) and the directed lines joining them (L_j , shown by the arrowed curves).

We see from the figure that every pair of points is connected uniquely by one of the lines,

to which belongs yet another (but only one) of the points. Conversely, every pair of lines intersects at a unique point, and one other line also shares this intersection. A more subtle property of this geometry (implied by the multiplicative Galois field structure) is the fact that we can increment uniformly all the point and line labels, modulo-7, and the structure of the configuration remains unchanged. A structural symmetry of this kind is an example of an ‘*automorphism*’. Thus, one group of automorphisms is isomorphic to C_7 , the cyclic group of order 7. This group of operations also preserves the cyclic ordering of the three points on each line, a directionality indicated in the diagram by the arrows on each of the lines. Another group of direction-preserving automorphisms, more immediately obvious from the figure, is the cyclic group of order 3 corresponding to applications of the ‘squaring automorphism’, which replaces each point’s label in the figure by the square of that label, modulo-7. For the special configuration shown in Fig. 1, this corresponds to a rotation of the figure by increments of 120° , which clearly continues to preserve the cyclic ordering of the points around each line. These two subgroups of the complete group of the order-preserving automorphisms they generate, which we shall denote ‘ $\text{Aut}^+\{PG(2, 2)\}$ ’, do not commute, so the direct product of them (which *is* commutative, since both C_3 and C_7 are) does **not** characterize $\text{Aut}^+\{PG(2, 2)\}$ even though the order of the group $|\text{Aut}^+\{PG(2, 2)\}| = 3 \times 7 = 21$. However, within this group, the right and left cosets of the subgroup of C_7 are the same (sets $C_7g = gC_7$ for each $g \in \text{Aut}^+\{PG(2, 2)\}$), making C_7 (but not C_3 !) the ‘*normal subgroup*’ of the two factors, denoted, $C_7 \triangleleft \text{Aut}^+\{PG(2, 2)\}$. This allows us to formally characterize the order-preserving automorphism group as the ‘*semi-direct product*’:

$$\text{Aut}^+\{PG(2, 2)\} \cong C_7 \rtimes C_3. \quad (2.4)$$

The symmetries of this restricted group of automorphisms play a guiding role in the construction of the simplest representation of the Hexad algorithm, as we discuss later. We also note here that a semi-direct composition analogous to (2.4) defines a restricted automorphism group in the 4D case, with C_4 replacing C_3 and C_{15} replacing C_7 , and respecting the implied symmetries in that case provides us with the tool we need to construct the Decad algorithm in a well-organized and systematic manner; this will be discussed in a separate note. The larger group, $\text{Aut}\{PG(2, 2)\}$, of *unrestricted* automorphisms, whose operations do not necessarily preserve the cyclic ordering of points around lines (an example being an operation that mirror-reflects the figure 1) plays no role here, but we note for completeness that this larger group, which is usually referred to as ‘*the automorphism group*’ of $PG(2, 2)$, has order $|\text{Aut}\{PG(2, 2)\}| = 168$.

We can also invoke the ‘duality’ operation of switching the interpretation of ‘points’ and ‘lines’ but simultaneously reversing the ordering of the indices, and, again the logical structure of the Fano plane configuration remains the same. Note that, given a distinguished index, i , the indices of the lines that pass through the point i , together with the indices of the points that belong to line i , collectively exhaust the full set of seven indices (obviously, this is true regardless of which i we deem to be ‘distinguished’).

This traditional diagram of the Fano plane is a simple and compact representation, but it possesses the stylistic defect of failing to make obvious the fact that *all* the points are on an equal footing and the three-fold symmetry that we see by rotating the figure by 120° about the central point, 0, is not so immediately obvious when we mentally substitute one of the other points for the point that remains fixed. An alternative and equivalent picture in which

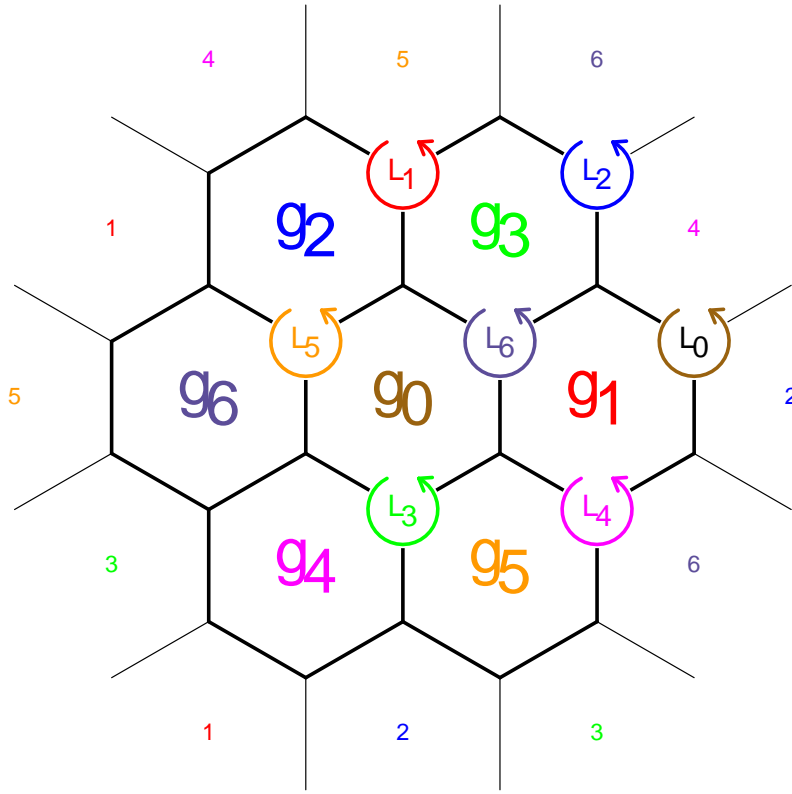


Figure 2. Alternative depiction of the Fano plane with seven points and the directed lines joining them (shown by the curly arrows).

this symmetry *is* obvious, is the hexagonal seven-tile symmetric covering of an appropriately proportioned torus, depicted ‘unwrapped’ in Fig. 2 as a doubly-periodic planar map. Here, the ‘points’ are represented by each of the seven sets of the replicated hexagonal tiles of each number from 0 to 6. The ‘lines’ are represented by the junctions of the seven indicated clusters of three hexagons that meet where the curly arrows show the cyclic ordering corresponding to that shown in Fig. 1. The further visual advantage of this alternative depiction is that, in addition to showing the three-fold periodicity about any point, it shows equally that there is a definite cyclic ordering and three fold periodicity about any chosen ‘line’.

Inspired by the connection relating the lattice-associated Galois field to the Fano geometry, we next elaborate on the structure of a hexad algorithm for the resolution of a given aspect tensor into its projected line-filter ‘weights’ (1D grid-relative aspect tensor components aligned with the orientation of each generalized line of the grid). As we shall see, the most elegant and symmetrical way to formulate the algorithm is to incorporate the symmetries exhibited by the Fano plane.

3. THE HEXAD ALGORITHM FORMULATED ACCORDING TO THE SYMMETRIES OF THE FANO GEOMETRY

As described in Purser et al. (2003b) each valid ‘hexad’ comprises a set of six integer 3-vector line-generators which, when augmented by their negatives, collectively form the twelve vertices of a squashed or distended cuboctahedron. This is equivalent to saying that this augmented set form the twelve midpoints of all the edges of a centered parallelepiped. Since a parallelepiped has eight vertices that we can write:

$$\{\pm\mathbf{a}, \pm\mathbf{b}, \pm\mathbf{c}\}, \quad (3.1)$$

each hexad therefore contains four distinct triads (not counting their negatives), of integer 3-vectors, which we shall denote:

$$\mathbf{L}_p \equiv \{\mathbf{a} - \mathbf{b}, \mathbf{b} - \mathbf{c}, -\mathbf{a} + \mathbf{c}\} \quad (3.2a)$$

$$\mathbf{L}_q \equiv \{\mathbf{a} - \mathbf{b}, \mathbf{b} + \mathbf{c}, -\mathbf{a} - \mathbf{c}\} \quad (3.2b)$$

$$\mathbf{L}_r \equiv \{\mathbf{a} + \mathbf{b}, -\mathbf{b} + \mathbf{c}, -\mathbf{a} - \mathbf{c}\} \quad (3.2c)$$

$$\mathbf{L}_s \equiv \{\mathbf{a} + \mathbf{b}, -\mathbf{b} - \mathbf{c}, -\mathbf{a} + \mathbf{c}\}. \quad (3.2d)$$

These correspond geometrically to the four bisecting planes that each contain six vertices (each comprising a triad of generators and their negatives) of the cuboctahedron. If we suppose the ‘color’ of the hexad (i.e., the color missing from its generators) conforming to the symmetry conventions of the Fano plane to be 0, we know that the colors of the four triads must be the Fano plane’s ‘lines’, $\mathcal{L}_0 = \{g_1, g_2, g_4\}$, $\mathcal{L}_1 = \{g_2, g_3, g_5\}$, $\mathcal{L}_2 = \{g_3, g_4, g_6\}$, and $\mathcal{L}_4 = \{g_5, g_6, g_1\}$, since these are the *only* ‘lines’ that do not contain the nonexistent g_0 of this hexad of color 0. We can always choose the signs of the six generators of the hexad of color 0 such that

$$\mathbf{g}_1 = \mathbf{g}_6 - \mathbf{g}_5 \quad (3.3a)$$

$$\mathbf{g}_2 = \mathbf{g}_5 - \mathbf{g}_3 \quad (3.3b)$$

$$\mathbf{g}_4 = \mathbf{g}_3 - \mathbf{g}_6, \quad (3.3c)$$

and organize the hexad of this color 0 into a tableau of the two-matrix form,

$$\begin{bmatrix} \mathbf{K}_0 \\ \mathbf{L}_0 \end{bmatrix} = \begin{bmatrix} (\mathbf{g}_6, \mathbf{g}_5, \mathbf{g}_3) \\ (\mathbf{g}_1, \mathbf{g}_2, \mathbf{g}_4) \end{bmatrix}. \quad (3.4)$$

A schematic sketch of this hexad is given in Fig. 3a, forming the corners of a squashed cuboctahedron inscribed in the lattice of generators. More generally, if the ‘color’ of the hexad is j , the corresponding tableau will comprise the two-matrix form:

$$\begin{bmatrix} \mathbf{K}_j \\ \mathbf{L}_j \end{bmatrix} = \begin{bmatrix} (\mathbf{g}_{j+6}, \mathbf{g}_{j+5}, \mathbf{g}_{j+3}) \\ (\mathbf{g}_{j+1}, \mathbf{g}_{j+2}, \mathbf{g}_{j+4}) \end{bmatrix}. \quad (3.5)$$

We note that the first row, or what we shall call the ‘K-set’, comprises the elements whose indices are those of the Fano lines that pass through the **point** indexed with the color index of the hexad (j , in this example), while the second row, or ‘L-set’, comprises the elements whose

indices are those of the Fano points that belong to the **line** with the index of the hexad. Also note that the ‘average’ (modulo-7) of the indices of the generators in each of the two rows of the tableau of (3.5) is always j , and the average in each column of the tableau is also always j itself, the hexad’s color. (This makes it very easy to deduce the colors of all the generators (and the color of the hexad itself) knowing only the color of one of the generators.)

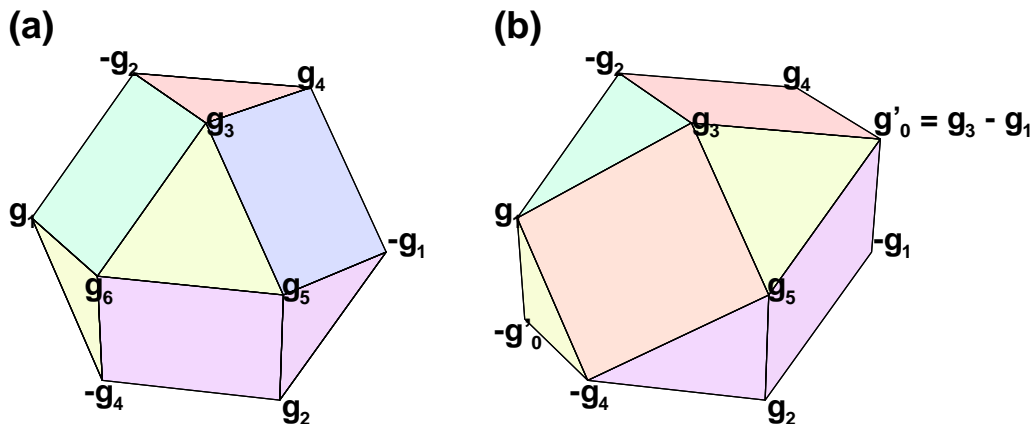


Figure 3. Schematic hexad of ‘color’ 0 (panel a), and the neighboring hexad of ‘color’ 6 (panel b) obtained by the single iteration of the hexad algorithm that discards old vertex, g_6 , and incorporates into the new hexad the vertex (of color 0) we call ‘ g'_0 ’.

Since each pattern of elements in the K and L rows of the tableau are also collectively cyclic over the three entries, the transition rules we use to iterate the choice of hexad in search of the one that resolves a given hexad into six positive line-smoothing weights can also be made conveniently cyclic with this same period-three restriction, systematizing and somewhat simplifying the algorithm, as we discuss next.

The 3D aspect tensor, \mathbf{A} , is symmetric, and therefore requires six independent values to specify it. The iterative preliminary step in the Hexad algorithm aims to find the unique hexad (set of six generators structured and organized as we have discussed above) so that, when the aspect tensor is projected onto the outer products of the six generators of the hexad, the resulting 6-vector of weights, \mathbf{W} , has only non-negative (and generally positive) components:

$$\mathbf{A} = \sum_j \mathbf{g}_j \mathbf{g}_j^T W_j, \quad W_j \geq 0. \quad (3.6)$$

If we assume the omitted generator that has the same index as the color of the hexad itself to be just the null vector, and its associated weight W_j to be zero, we can conveniently let the indices j in (3.6) range over *all* of the colors, 0 — 6. The iteration that resolves the hexad in this way proceeds from an arbitrary starting valid guess hexad, and examines the weights \mathbf{W} that come from the projection of the aspect tensor onto its generators as in (3.6). Typically, the guess is not the correct hexad for this aspect tensor, \mathbf{A} , and one or more of the weights W_j will be found to be negative – in which case, the algorithm picks the one which possesses the minimum (most negative) value, and determines whether its index corresponds to one from the K-set, or one from the L-set.

(a) *Transition removing a generator from the K-set*

In the case that the generator belongs to the K-set, then, let us suppose it is the *first* member, i.e., \mathbf{g}_{j+6} for a hexad of color index j . The color of the hexad is clearly changed to this same $j + 6$. The new matrix, \mathbf{K}'_{j+6} , of generators comprising the K-set after the needed corrective step, is defined from the old K-matrix, \mathbf{K}_j , by the rule:

$$\mathbf{K}'_{j+6} = \mathbf{K}_j \mathbf{M}_6, \quad (3.7)$$

where the matrix, \mathbf{M}_6 , that causes a transition that replaces element \mathbf{g}_{j+6} is, by the cyclic symmetry inherited from the Fano geometry, independent of j and is defined:

$$\mathbf{M}_6 = \begin{bmatrix} 0 & 1 & 0 \\ 1 & 0 & 1 \\ 0 & -1 & -1 \end{bmatrix}. \quad (3.8)$$

In terms of the explicit component generators, this rule is equivalent to:

$$\mathbf{K}'_{j+6} \equiv [\mathbf{g}'_{j+5}, \mathbf{g}'_{j+4}, \mathbf{g}'_{j+2}] = [\mathbf{g}_{j+5}, \mathbf{g}_{j+6} - \mathbf{g}_{j+3}, \mathbf{g}_{j+5} - \mathbf{g}_{j+3}], \quad (3.9)$$

and since we must maintain the corresponding L-set of generators to continue to satisfy the linear relationship corresponding (indices modulo-7) to (3.3a) — (3.3b), which in matrix form is just,

$$\mathbf{L} = \mathbf{K} \mathbf{N}, \quad (3.10)$$

for *any* associated pair of \mathbf{L} and \mathbf{K} matrices, where,

$$\mathbf{N} = \begin{bmatrix} 1 & 0 & -1 \\ -1 & 1 & 0 \\ 0 & -1 & 1 \end{bmatrix}, \quad (3.11)$$

we find that the new L-set after the transition that replaces the old generator of color $j + 6$ has for its members the columns of the new matrix:

$$\mathbf{L}'_{j+6} \equiv [\mathbf{g}'_j, \mathbf{g}'_{j+1}, \mathbf{g}'_{j+3}] = [-\mathbf{g}_{j+6} + \mathbf{g}_{j+5} + \mathbf{g}_{j+3}, \mathbf{g}_{j+6} - \mathbf{g}_{j+5}, -\mathbf{g}_{j+3}]. \quad (3.12)$$

In Fig. 3 an example of the transition of exactly this kind is illustrated in the step that takes the hexad of panel (a) of the figure into the new hexad of panel (b). The cuboctahedral shape is clearly preserved, although it becomes squashed in a slightly different way.

Note that, had it been either the second or third elements, \mathbf{g}_{j+5} or \mathbf{g}_{j+3} , that needed to be replaced, then we should have used, in place of matrix \mathbf{M}_6 to effect the transition, the matrices \mathbf{M}_5 or \mathbf{M}_3 instead (also independent of j), where

$$\mathbf{M}_5 = \begin{bmatrix} -1 & 0 & -1 \\ 0 & 0 & 1 \\ 1 & 1 & 0 \end{bmatrix}, \quad \mathbf{M}_3 = \begin{bmatrix} 0 & 1 & 1 \\ -1 & -1 & 0 \\ 1 & 0 & 0 \end{bmatrix}. \quad (3.13)$$

(These are simply cyclic rotations, of both rows and columns, of \mathbf{M}_6 itself.) Note the period-3 cyclic sequence of \mathbf{M} -indices, or relative to j , the generator indices, involves a successive

doubling, modulo-7, which corresponds to the ‘squaring automorphisms’ in the subgroup C_3 of $\text{Aut}^+\{PG(2, 2)\}$, or course. The cyclic additive increments, modulo-7, of the hexad color index, j , corresponds to automorphisms that belong to the subgroup, C_7 , as discussed in section 2.

(b) *Transition removing a generator from the L-set*

Let us now consider the form of the transition that occurs when it is one of the elements, say \mathbf{g}_{j+1} , of the L-set that needs to be replaced. In this example, the new hexad will have the color index of the index of the replaced generator, $j + 1$, and so the new K-set matrix of generators will be denoted \mathbf{K}'_{j+1} . The rule that generates it in this case is:

$$\mathbf{K}'_{j+1} = \mathbf{K}_j \mathbf{M}_1, \quad (3.14)$$

where

$$\mathbf{M}_1 = \begin{bmatrix} 1 & 1 & 1 \\ 1 & 0 & 0 \\ -1 & 0 & -1 \end{bmatrix}, \quad (3.15)$$

and the new L-set, \mathbf{L}'_{j+1} , will be given by the corresponding equation of the form (3.10). As before, if other elements of the original L-set need to be replaced instead, \mathbf{g}_{j+2} or \mathbf{g}_{j+4} , then the matrices \mathbf{M}_2 or \mathbf{M}_4 for the transition are cyclic rotations of the rows and columns of \mathbf{M}_1 . Explicitly:

$$\mathbf{M}_2 = \begin{bmatrix} -1 & -1 & 0 \\ 1 & 1 & 1 \\ 0 & 1 & 0 \end{bmatrix}, \quad \mathbf{M}_4 = \begin{bmatrix} 0 & 0 & 1 \\ 0 & -1 & -1 \\ 1 & 1 & 1 \end{bmatrix}. \quad (3.16)$$

Note the period-3 cyclic sequence of \mathbf{M} -indices, or relative to j , the generator indices, again involves a successive doubling, modulo-7, of the color index, corresponding to the squaring automorphism, C_3 , of the Galois field elements that represent the ‘points’ of the Fano plane.

4. REMARKS

An alternative presentation of the rules governing the six possible transitions out of one hexad and into one of its neighbors is provided in the appendix, using just the three component generators of the initial K-set exemplified by a \mathbf{K}_0 for the color-0 case (since cyclic rotation of the indices of the \mathbf{g} automatically provides the correct transition rules for the other cases). In the alternative presentation, the period-3 symmetries become more easily apparent.

In practice, several iterative steps of these K-set or L-set transition rules need to occur before the vector of weights \mathbf{W} has all its components non-negative (generally, one component of this 7-vector, the component corresponding to the final hexad’s own color, will be exactly zero and the rest will usually all be positive.) Excepting special non-generic borderline cases, the resulting hexad is unique, regardless of the point of departure for this iteration. An examination of the implications of the hexad algorithm constructed in this maximally symmetric form reveals that these transitions ensure that:

(i) The change from hexad color j to color k , followed by the reverse transition back to color j , leaves the final hexad of generators identical (including signs) to the original (invariance with respect to double-transpositions, or circuits of period two, in the space of hexads).

(ii) If colors i , j and k belong to a triad (e.g., if $j = i + 1$ and $k = i + 3$, modulo-7) then a transition from a hexad of color i , to one of color j followed by a transition to one of color k , and finally to color i , returns the hexad to its original state and preserves the signs of the generators (invariance with respect to circuits of period three).

(iii) If a sequence of six transitions (such as the transitions from a hexad of color j to $j + 6$, $j + 1$, j , $j + 6$, $j + 1$, j , for example) that return the hexad back to its original, then, again, the signs of each generator remain unchanged (invariance with respect to circuits of period six).

A careful study of the network formed by all the adjacent hexads reveals that its irreducible cycles comprise *only* those of periods two, three and six, so it seems that our Fano-inspired version of the Hexad algorithm has the admirable property of always producing any given hexad in a unique configuration of its signed generators (which was not true of previous implementations of the hexad algorithm) provided the starting point of the iterations is always either the same, or else some other hexad previously derived from that same starting point.

5. SUMMARY AND DISCUSSION

We have described a new formulation of the ‘Hexad Algorithm’ for decomposing a given 3D symmetric positive-definite aspect tensor on a lattice into its six unique local line generators and corresponding projected rank-one aspect tensor contributions. The new formulation adheres strictly to the symmetries possessed by the associated Fano projective plane and Galois field, $GF(8)$. A bonus of adopting these constraints is that the computer code in the new algorithm is relatively succinct.

The motivation for this work has been to provide a supporting algorithmic framework for the production of a computationally efficient way to generate anisotropic and spatially inhomogeneous covariances, initially for NOAA’s new 3D RTMA, but also for more general data assimilation applications later. The rank-one components of the aspect tensor are dealt with using quasi-Gaussian line filters. In the past the line filters used in NCEP’s Grid-point Statistical Interpolation have been the ‘recursive filters’ (Wu et al., 2002). More recently, an effort has been made to replace those line filters by compact-support beta distribution lines filters, which are also of quasi-Gaussian form, but which are better suited for efficient parallelization. Another technical distinction between the recursive filters and the beta filters is that the former are self-adjoint but are neither perfectly conserving nor perfect (value-preserving) smoothers in inhomogeneous conditions, while the latter filters, come in two mutually-adjoint forms, one of which is perfectly conserving, and its adjoint is a perfect value-preserving filter (when applied to a constant-value field) regardless of the spatial anisotropy of the aspect tensor. It appears that these complementary attributes of the mutually-adjoint forms of the new beta filters enables them to combine sequentially within algorithms of the Triad, Hexad, or Decad type, in such a way that the complete self-adjoint combination suffers no visible numerical noise at the boundaries between one polyad’s spatial domain and the next; this was not the case when employing the recursive filters, and necessitated additional measures (such as the replacement of the basic Triad algorithm with the more complicated ‘Blended Triads’ method employed in the present 2D RTMA) in order to avoid the numerical noise.

ACKNOWLEDGMENTS

The author is grateful to Drs. Kristen Bathmann, Manuel Pondeca, and Styliano Flampouris, for their helpful reviews.

APPENDIX A

Summary of hexad transition rules in a notation that exhibits the C_3 symmetry

Without loss of generality, we can assume that the color of the initial hexad is 0, since, if it is any other color, we need only appropriately increment (modulo-7) the color indices of the generators, \mathbf{g} , to acquire the transition rules in other cases. With this assumption, we might also want to see the structure of the transition rules that gives a clearer emphasis to the inherent period-3 structure that they possess, so, to this end, we alias the generators of the original K-set, \mathbf{K}_0 , as follows:

$$\mathbf{v}_0 = \mathbf{g}_6 \tag{A.1a}$$

$$\mathbf{v}_1 = \mathbf{g}_5 \tag{A.1b}$$

$$\mathbf{v}_2 = \mathbf{g}_3, \tag{A.1c}$$

so that the tableau of the starting color-0 hexad, and the corresponding matrix of colors of its generators, are:

$$\begin{bmatrix} \mathbf{K}_0 \\ \mathbf{L}_0 \end{bmatrix} = \begin{bmatrix} \mathbf{v}_0, & \mathbf{v}_1, & \mathbf{v}_2 \\ \mathbf{v}_0 - \mathbf{v}_1, & \mathbf{v}_1 - \mathbf{v}_2, & \mathbf{v}_2 - \mathbf{v}_0 \end{bmatrix} \quad \mathbf{C}_0 = \begin{bmatrix} 6 & 5 & 3 \\ 1 & 2 & 4 \end{bmatrix}. \tag{A.2}$$

Then, in terms of these three initial generators, \mathbf{v} , the hexads obtained by making transitions to neighbors of each of the colors other than 0, taken in the order that these colors present themselves in the original hexad's tableau, and the colors in these new tableaux, are as follows:

$$\begin{bmatrix} \mathbf{K}_6 \\ \mathbf{L}_6 \end{bmatrix} = \begin{bmatrix} \mathbf{v}_1, & \mathbf{v}_0 - \mathbf{v}_2, & \mathbf{v}_1 - \mathbf{v}_2 \\ -\mathbf{v}_0 + \mathbf{v}_1 + \mathbf{v}_2, & \mathbf{v}_0 - \mathbf{v}_1, & -\mathbf{v}_2 \end{bmatrix} \quad \mathbf{C}_6 = \begin{bmatrix} 5 & 4 & 2 \\ 0 & 1 & 3 \end{bmatrix} \tag{A.3a}$$

$$\begin{bmatrix} \mathbf{K}_5 \\ \mathbf{L}_5 \end{bmatrix} = \begin{bmatrix} -\mathbf{v}_0 + \mathbf{v}_2, & \mathbf{v}_2, & -\mathbf{v}_0 + \mathbf{v}_1 \\ -\mathbf{v}_0, & \mathbf{v}_0 - \mathbf{v}_1 + \mathbf{v}_2, & \mathbf{v}_1 - \mathbf{v}_2 \end{bmatrix} \quad \mathbf{C}_5 = \begin{bmatrix} 4 & 3 & 1 \\ 6 & 0 & 2 \end{bmatrix} \tag{A.3b}$$

$$\begin{bmatrix} \mathbf{K}_3 \\ \mathbf{L}_3 \end{bmatrix} = \begin{bmatrix} -\mathbf{v}_1 + \mathbf{v}_2, & \mathbf{v}_0 - \mathbf{v}_1, & \mathbf{v}_0 \\ -\mathbf{v}_0 + \mathbf{v}_2, & -\mathbf{v}_1, & \mathbf{v}_0 + \mathbf{v}_1 - \mathbf{v}_2 \end{bmatrix} \quad \mathbf{C}_3 = \begin{bmatrix} 2 & 1 & 6 \\ 4 & 5 & 0 \end{bmatrix} \tag{A.3c}$$

$$\begin{bmatrix} \mathbf{K}_1 \\ \mathbf{L}_1 \end{bmatrix} = \begin{bmatrix} \mathbf{v}_0 + \mathbf{v}_1 - \mathbf{v}_2, & \mathbf{v}_0, & \mathbf{v}_0 - \mathbf{v}_2 \\ \mathbf{v}_1 - \mathbf{v}_2, & \mathbf{v}_2, & -\mathbf{v}_1 \end{bmatrix} \quad \mathbf{C}_1 = \begin{bmatrix} 0 & 6 & 4 \\ 2 & 3 & 5 \end{bmatrix} \tag{A.3d}$$

$$\begin{bmatrix} \mathbf{K}_2 \\ \mathbf{L}_2 \end{bmatrix} = \begin{bmatrix} -\mathbf{v}_0 + \mathbf{v}_1, & -\mathbf{v}_0 + \mathbf{v}_1 + \mathbf{v}_2, & \mathbf{v}_1 \\ -\mathbf{v}_2, & -\mathbf{v}_0 + \mathbf{v}_2, & \mathbf{v}_0 \end{bmatrix} \quad \mathbf{C}_2 = \begin{bmatrix} 1 & 0 & 5 \\ 3 & 4 & 6 \end{bmatrix} \tag{A.3e}$$

$$\begin{bmatrix} \mathbf{K}_4 \\ \mathbf{L}_4 \end{bmatrix} = \begin{bmatrix} \mathbf{v}_2, & -\mathbf{v}_1 + \mathbf{v}_2, & \mathbf{v}_0 - \mathbf{v}_1 + \mathbf{v}_2 \\ \mathbf{v}_1, & -\mathbf{v}_0, & \mathbf{v}_0 - \mathbf{v}_1 \end{bmatrix} \quad \mathbf{C}_4 = \begin{bmatrix} 3 & 2 & 0 \\ 5 & 6 & 1 \end{bmatrix}. \tag{A.3f}$$

REFERENCES

- De Pondaca, M. S. F. V., and Coauthors 2011 The Real-Time Mesoscale Analysis at NOAA's National Centers for Environmental Prediction: Current Status and Development. *Wea. Forecasting*, **26**, 593-612.
- Fano, G. 1892 Sui postulati fondamentali della geometria proiettiva in uno spazio lineare a un numero qualunque di dimensioni. *Giornale di Matematiche*, **30**, 106-132.
- Hayden, C. M., and R. J. Purser 1995 Recursive filter objective analysis of meteorological fields: applications to NESDIS operational processing. *J. Appl. Meteor.*, **34**, 3-15.
- Purser, R. J. 2020 A formulation of the Decad algorithm using the symmetries of the Galois field, $GF(16)$. NOAA/NCEP Office Note 500.
- Purser, R. J., and R. McQuigg 1982 A successive correction analysis scheme using recursive numerical filters. Met. O 11 Tech. Note, No. 154, British Meteorological Office. 17 pp.
- Purser, R. J., W.-S. Wu, D. F. Parrish, and N. M. Roberts 2003a Numerical aspects of the application of recursive filters to variational statistical analysis. Part I: Spatially homogeneous and isotropic Gaussian covariances. *Mon. Wea. Rev.*, **131**, 1524-1535.
- Purser, R. J., W.-S. Wu, D. F. Parrish, and N. M. Roberts 2003b Numerical aspects of the application of recursive filters to variational statistical analysis. Part II: Spatially inhomogeneous and anisotropic general covariances. *Mon. Wea. Rev.*, **131**, 1536-1548.
- Veblen, O., and W. H. Bussey 1906 Finite projective geometries. *Trans. Amer. Math. Soc.*, **7**, 241-259.
- Wu, W.-S., R. J. Purser, and D. F. Parrish 2002 Three-dimensional variational analysis with spatially inhomogeneous covariances. *Mon. Wea. Rev.*, **130**, 2905-2916.